Live imaging of synapse development and measuring protein dynamics using two-color fluorescence recovery after photo-bleaching at *Drosophila* synapses

Petra Füger[1], Laila B Behrends[1], Sara Mertel[2], Stephan J Sigrist[2] & Tobias M Rasse[1]

[1]Department of Cellular Neurology, Hertie Institute for Clinical Brain Research, University of Tübingen, Otfried-Müller Strasse 27, Tübingen D-72076, Germany. [2]Institut für Klinische Neurobiologie und Rudolf-Virchow-Zentrum Universität Würzburg Zinklesweg 10, Würzburg D-97078, Germany. Correspondence should be addressed to T.M.R. (tobias.rasse@medizin.uni-tuebingen.de).

Published online 13 December 2007; doi:10.1038/nprot.2007.472

Here we describe how to anesthetize and image *Drosophila* larvae as to follow 'the life history' of identified synapses and synaptic components. This protocol is sensitive, for example, the distribution of glutamate receptors expressed at physiological levels can be monitored. Typically, 2–20 time points can be recorded in the intact organism. Finally, we discuss how to extract the kinetic information on protein dynamics from two-color fluorescence recovery after photo-bleaching (FRAP) measurements and give advice how to keep the *in vivo* imager's five arch enemies—limited temporal and spatial resolution, injury of the animal, inactivation of proteins and movement artifacts—in check. While we focus on synapses, as model structure, the protocol can easily be adapted to study other developmental processes such as muscle growth, gut development or tracheal branching.

INTRODUCTION

Our nervous system is dynamic; it changes constantly. Thus, it is difficult to attempt understanding its cellular function without comprehending the individual steps, by which its most basic units—synapses—are constructed, stabilized and eliminated. Such dynamics are ideally studied by following the trafficking of individual synaptic components expressed at physiological levels in the intact organism at single synapse resolution. While first attempts in that direction have already been taken at the vertebrate neuromuscular junction (NMJ)[1], and very recently also in the mammalian CNS[2], we describe how and why we use *Drosophila* for *in vivo* imaging of synapses and their components[3]. At the *Drosophila* NMJ electrophysiological protocols are well established, ultrastructure is thoroughly described and genetic accessibility allows functional manipulation of gene products specifically at either the presynaptic or the postsynaptic site. *Drosophila* NMJs are structurally plastic[4], and in terms of function and structure similar to the excitatory synapses of the vertebrate CNS. *Drosophila* larvae are transparent and have a stereotyped cytoarchitecture of muscles and neurons. Thus, they are ideally suited for *in vivo* imaging. Consequently, it was a long-standing goal to establish *in vivo* imaging to make a powerful model organism even more attractive.

Despite many efforts, only two studies describing the *in vivo* imaging of *Drosophila* larvae have been published so far[3,5]. In a landmark study, Zito and colleagues imaged the development of the bouton structure at identified NMJs over the time-course of days *in vivo*[5]. To image individual synapses, that is, the transmitter release sites including active zones and their apposed glutamate receptor clusters, the degree of anesthetization is absolutely crucial. Any residual heartbeat will reduce the image quality substantially. At the same time, a deep anesthetization must not affect the survival rate negatively. Thus, we developed and initially described a protocol[3] that addressed three key issues: degree of anesthetization, survival rate and sensitivity.

1. *Degree of anesthetization. Drosophila* larvae move strongly; thus, live imaging of individual identified synapses critically demands stable anesthetization. Desflurane anesthetization is so strong that even the heartbeat arrests. Therefore, the maximal resolution is only limited by the physical properties inherent to the microscope used.
2. *Survival rate.* The use of ether to anesthetize larvae[5] led, in our hands, to a substantial mortality rate. Thus, we switched to volatile application of desflurane. Control experiments consisting of ten consecutive desflurane anesthetizations, separated by 5-min recovery intervals, revealed neither any developmental delay nor increased mortality in anesthetized larvae compared to nonanesthetized, but otherwise identically treated sibling larvae[6].
3. *Sensitivity.* Our protocol allows us to follow the dynamics of synaptic components—for example, postsynaptic glutamate receptors[7] and presynaptic calcium channels[8]—in an intact, living organism. The imaging procedure is sensitive enough that usually no overexpression of the protein of interest is necessary. As exemplified in Rasse and colleagues[3], the turnover of glutamate receptors, expressed by their endogenous promoter at physiological levels, can be visualized.

Overview of procedure

We detail the imaging protocol in the Image Acquisition section. Technically, the volatile application of several pulses of a desflurane/air mixture to *Drosophila* larvae mounted in an imaging chamber allows for repetitive imaging. As intact larvae are imaged, the protein of interest is to be tagged by suitable fluorescent labels, ideally by fusion with green or red fluorescent proteins that do not aggregate substantially (for review, see ref. 9). For a list of particular useful transgenic lines, see **Figure 1** and **Tables 1** and **2**. Recent improvements in the sensitivity of confocal microscopes and novel transgenic constructs[8,10] now allow the extension of these analyses

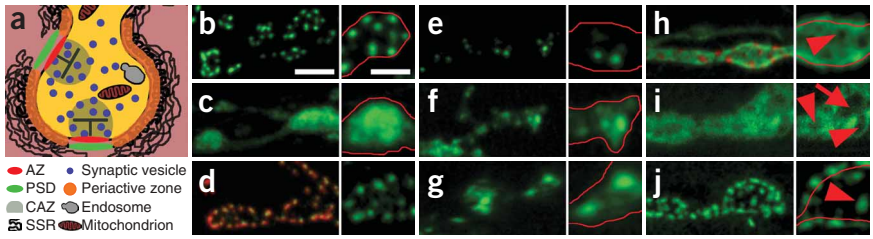

Figure 1 | Transgenic lines particularly useful for *in vivo* imaging. (**a**) Schematic overview of a single presynaptic type 1 bouton (yellow) embedded in a third instar larval body wall muscle (pink). The muscle membrane folds into a specialized structure called the subsynaptic reticulum (SSR), which is similar to junctional folds at the vertebrate neuromuscular junction (NMJ). Each bouton usually contains 10–20 synapses that are characterized by a postsynaptic density (PSD) opposing the presynaptic active zone (AZ). One main feature of the cytomatrix of AZ (CAZ) is a dense projection, the so-called T bar. Synapses are surrounded by the periactive zone (orange). (**b**–**j**) Examples of transgenic constructs (green channel) that can be utilized to visualize the structures and compartments depicted in (**a**). GluRIIA$^{mRFP\,3}$ was used to mark the PSDs (red channel in (**d**) and (**h**)). Shown are projections of confocal stacks of mid-third instar larva. Scale bar is 4 μm. The red line in the right panel in (**b**), (**c**), (**e**–**h**) and (**j**) indicates the position of the presynaptic membrane. Scale bar for right panel: (**b**–**h**) and (**j**) 2 μm, for (**i**) 4 μm. The right panel in (**i**) shows a projection of ~2 μm out of the central part of a synaptic bouton to better visualize the position of synapses (arrowheads) and of the presynaptic cytosol (arrow). The arrowheads in (**h**) and (**j**) point likewise at the position of synapses, which are characterized by the absence of the periactive zone marker Fasciclin 2 (**h**) and the presence of the PSD marker PAK (**j**). (**b**) Ok6-Gal4 > Bruchpilot-GFP[10] depicts the CAZ. (**c**) D42-Gal4 > Synaptotagmin-GFP[17] visualizes synaptic vesicles. (**d**) Elav^{C155}-Gal4 > Cacophony-GFP[8] localizes to the AZ. (**e**) Ok6-Gal4 > GFP-2xFYVE-GFP[18] marks early endosomes. (**f**) Ok6-Gal4 > Actin 5C-GFP can be used as cytoskeleton marker. (**g**) D42-Gal4 > Mito-GFP[19] visualizes mitochondria. (**h**) Fasciclin2-GFP[3] marks the periactive zone. (**i**) Mhc^{-82} > mCD8-GFP-Shaker visualizes the SSR[5]. (**j**) G14-Gal4 > PAK-GFP[3] localizes to PSDs. (**d**) Adapted from ref. 3.

to study simultaneously presynaptic and postsynaptic assembly. It is noteworthy that the protocols for anesthetization and imaging are not limited to studying NMJs. In combination with the appropriate fluorescent protein (FP) fusion constructs, it can easily be adapted to study a large variety of developmental or pathological processes in *Drosophila* larvae.

Next, we describe how the combination of two-color fluorescence recovery after photo-bleaching (FRAP) with *in vivo* imaging allows us to measure turnover, synaptic residence times, directed transport and passive diffusion of proteins. Why two colors? The first color will be used for bleach and recovery analyses. The availability of an unbleached reference channel provides additional information on the steady-state distribution of proteins. Many changes in the cytoarchitecture—such as the formation of new synapses—may occur during long-term imaging experiments. Such changes can be monitored in the unbleached reference channel to then state, for example, that a certain protein is preferably incorporated into new synapses and is lost soon after their stabilization. To perform a two-color FRAP experiment, two prerequisites are mandatory. The protein of interest has to be tagged with two different fluorophores, FP1 and FP2, for example, GFP and mCherry. It is possible to attach two fluorescent tags to a single protein. We typically tag one fraction of the protein population with FP1 and another fraction with FP2 out of concern that two tags might be more likely to disrupt the proteins function than just a single one. For this aim, two independent transgenic lines have to be established and crossed. In the progeny where both transgenes are combined, FP1 can be selectively bleached, while the FP2 signal serves as reference. This type of bleaching typically does not affect the function of the tagged protein. FRAP, as described here, can be adapted to study many biological processes and is not limited to study protein turnover at the *Drosophila* NMJ.

Finally, we give a comprehensive description of how to process imaging data as to extract quantitative information. Changes in overall morphology, differences in spatial orientation at various time points and the fact that synapses are closely spaced interfere with fully automated detection and quantification. While technical improvements would facilitate processing substantially, we currently still recommend manual image processing using ImageJ. We will highlight in the Image processing and quantification section all crucial image-processing steps necessary to extract accurate quantitative information.

MATERIALS

REAGENTS

- Fly stocks (see **Fig. 1**, **Tables 1** and **2**)
- Desflurane (Suprane; Baxter) **! CAUTION** Acute exposure may cause eye and skin irritation. Overexposure by inhalation can lead to headaches, dizziness, drowsiness, unconsciousness or death.
- Halocarbon oil (e.g., Voltalef H10S oil; Atofina)
- Fly cultivation medium

EQUIPMENT

- Inverted confocal microscope (we use primarily a Zeiss Axiovert 200M microscope equipped with a LSM 510 scanhead (Carl Zeiss) and a Leica DM IRE2 microscope equipped with a TCS SP2 AOBS scanhead and an additional 10 mW 561-nm solid state laser (Leica Microsystems))
- Objective (e.g., Plan-Neofluar 40× oil 1.3 numerical aperture (NA) or Plan-Apochromat 63× oil 1.4 NA; Carl Zeiss)
- Binocular microscope (e.g., Stemi 2000; Carl Zeiss)
- Cover slip 22 × 22 mm^2 (Menzel-Gläser)
- Parafilm (Pechiney Plastic Packaging)
- Plastic Petri dish, diameter 55 mm height 13 mm (VWR International GmbH)
- Small (size 3) paintbrush as used to sort flies (Neolab GmbH)
- Incubator (e.g., KB720, Binder GmbH)
- Image-processing software (Image J version 1.37v; NIH) *Note*: All image processing described is done in ImageJ 1.37 v.
- Round cover slips, diameter 50 mm, thickness 0.12 mm (Menzel-Gläser)
- Glue (UHU)
- Silicone tubes (Neolab GmbH)
- Custom build imaging chamber (**Fig. 2a–k**; mechanical drawings see **Supplementary Figs. 1–7** online)
- Vaporizer/anesthetization device: custom-made (**Fig. 2l** and **m**) or commercial (e.g., Dräger or GE Healthcare; ask for low air-flow rates <50 ml min^{-1}) **! CAUTION** For safety reasons, we strongly recommend to buy a commercial vaporizer. Do not build your own anesthetization device, unless you are professionally trained.
- Modified Petri dish (see EQUIPMENT SETUP)
- Plastic spacer 22 × 22 mm^2 (see EQUIPMENT SETUP)
- Plexiglas guide ring (see EQUIPMENT SETUP)
- Anodized metal ring (see EQUIPMENT SETUP)
- Plexiglas lid (see EQUIPMENT SETUP)

TABLE 1 | Useful fly stocks for *in vivo* imaging.

Protein	Tag	Cellular compartment	Remarks	Gal4-driver required	BDSC Stock#	Ref.
Bruchpilot	GFP	CAZ	Presynaptic scaffold, CAST homolog	Yes	—	10
Cacophony	GFP	AZ	Membrane marker, calcium channel α1-subunit	Yes	8580–8582	8
Synaptotagmin	GFP	Synaptic vesicle	Calcium dependent membrane targeting	Yes	6924–6926	17
Synaptobrevin	GFP	Synaptic vesicle		Yes	6921, 6922	17
Shaggy	GFP	Presynaptic	Glycogen synthase kinase-3beta (GSK-3beta) homolog; exon trap line	No	—	21
Rab-proteins (several)	GFP, YFP, RFP	Endosome	Markers for different endosomal stages	Yes	Several stocks	22
GFP-2xFYVE		Endosome	Early endosomes, construct contains only FYVE-domain	Yes	—	18
Mito-GFP		Mitochondrion	Construct containing a mitochondrial import sequence	Yes	8442, 8443	19
Actin 5C	GFP	Cytoskeleton	Actin 5C construct	Yes	7309–7311	
α-Tubulin at 84B	GFP	Cytoskeleton	α-Tubulin construct	Yes	7373, 7374	23
Fasciclin 2	GFP	Periactive zone	NCAM homolog; exon trap line	No	—	3
Basigin	GFP	Periactive zone	IgG family glycoprotein; exon trap line	No	—	24
Glutamate receptor IIA	GFP, RFP	Postsynaptic density (PSD)	Glutamate receptor subunit	No	—	3
PAK-kinase	GFP	PSD	P21-activated kinase (PAK) homolog	Yes	—	3
Discs large	GFP	SSR	PSD-95 homolog	Yes	—	20
CD8-GFP-Shaker		SSR	Chimeric construct of CD8 and Shaker potassium channel C-Term	No		5
mCD8-GFP		Plasma membrane	Membrane-targeted UAS-GFP construct (fusion to murine CD8 transmembrane domain)	Yes	5136, 5137	25
myr-RFP		Plasma membrane	UAS-monomeric RFP construct containing a myristoylation signal	Yes	7118, 7119	

Gal4-driver: Gal4-driver line required or not; BDSC stock#: official stock numbers from Bloomington Drosophila Stock Center (http://flystocks.bio.indiana.edu/). AZ: active zone; CAZ: cytomatrix of the AZ; RFP: red fluorescent protein; SSR: subsynaptic reticulum; YFP: yellow fluorescent protein.

EQUIPMENT SETUP

Modified Petri dish See **Figure 2a**, red arrow; for a mechanical drawing, see **Supplementary Figure 1.** Drill a 39 mm hole in the base plate of a 55 mm standard Petri dish. (**Fig. 2a**, red arrow; for a mechanical drawing, see **Supplementary Fig. 1**). Use strong glue to attach tightly a round cover slip (diameter 50 mm, thickness 0.12 mm) on the remaining border ▲ CRITICAL STEP Avoid air bubbles in order to achieve an airproof seal. **Plastic spacer 22 mm × 22 mm** containing a slit in its center (**Fig. 2a**, white arrow; mechanical drawing see **Supplementary Fig. 2**).

Plexiglas guide ring See **Figure 2a**, white arrowhead; for a mechanical drawing, see **Supplementary Figure 3**.

Anodized metal ring See **Figure 2a**, red arrowhead; for a mechanical drawing, see **Supplementary Figure 4**.

Plexiglas lid For a mechanical drawing, see **Supplementary Figure 5**. Contains three hose connections (for a mechanical drawing, see **Supplementary Fig. 6**) and an implemented *o*-ring (**Fig. 2b**, arrow) seal that forms a hermetical seal when the lid (assembly, see **Supplementary Fig. 7**) is put on the Petri dish (**Fig. 2c**).

PROCEDURE

Image acquisition: assemble the imaging chamber ● TIMING 5 min

1| Select a larva of chosen stage (e.g., early third instar larvae leaving an observation interval of ~24 h at 25 °C until wandering stage).

TABLE 2 | Useful Gal4-driver lines for *in vivo* imaging.

	Name	Expression pattern	BDSC Stock#	Ref.
Presynaptic	D42	Motoneurons	8816	26
	elav^{C155}	Enhancer trap in *elav* locus; all tissues of embryonic nervous system starting at stage 12	458	27
	elav^{3A4}	*elav* Promoter: Gal4 fusion inserted on the third chromosome; postmitotic neurons, all CNS and peripheral nervous system	—	28
	Ok6	All motoneurons, salivary glands, wing discs, and a subset of tracheal branches	—	29
	elav-GS	GeneSwitch; RU486 inducible neuronal Gal4 expression	—	30
Postsynaptic	24B	All embryonic muscles starting at stage 12 to the larval third instar	1767	31
	Mhc^{-82}	High levels, specifically in muscles at the first larval instar	—	32
	G14	All somatic muscles and salivary glands	—	29
	C57	Mesodermal driver line	—	33
	twist	Embryonic mesoderm starting at stage 8	914	34
	Mhc-GS	GeneSwitch; RU486 inducible Gal4 expression in muscles	—	30

BDSC stock#: official stock numbers from Bloomington Drosophila Stock Center (http://flystocks.bio.indiana.edu/).

▲ **CRITICAL STEP** Unless you want to study the effects of overexpression, it is most accurate to study your protein of interest when expressed at physiological levels. Ideally, each protein is expressed by its endogenous promoter. Alternatively, the Gal4-driver/temperature combination at which physiological expression levels can be obtained is to be chosen. Expression levels are to be measured; for example, by a western blot that detects simultaneously the native protein and the transgenically expressed GFP-tagged variant.

2| Rinse the larva with water and dab it dry to clean it of the cultivation medium.

3| Coat the center of the bottom part of the chamber (**Fig. 2a**, red arrow; **Fig. 2g**, orange part) that will face the larva with a thin film of Voltalef oil.

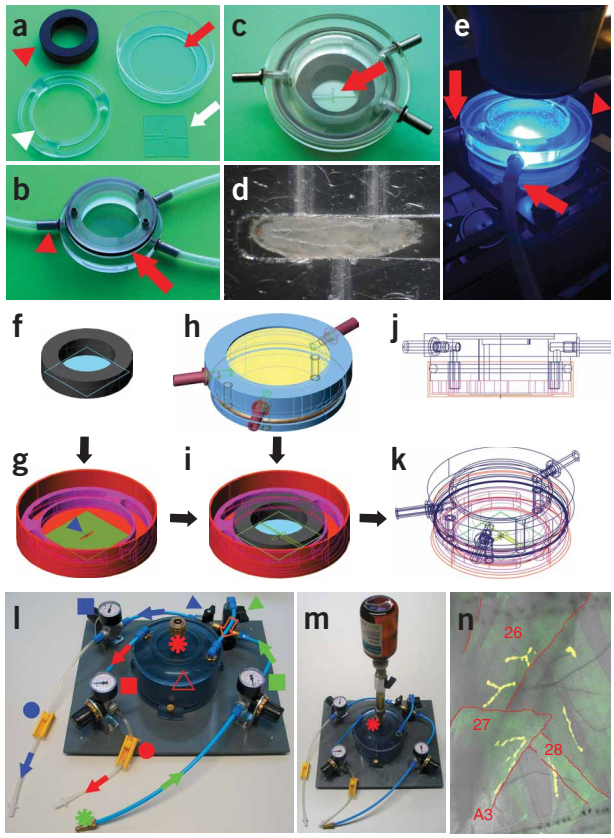

Figure 2 | Assembly of the imaging chamber. (**a**,**b**) Individual parts of the *in vivo* imaging chamber. (**a**) Anodized metal ring (red arrowhead), modified Petri dish (red arrow), Plexiglas guide ring (white arrowhead) and plastic spacer (white arrow). (**b**) Lid of the chamber. Hose connection (arrowhead) of the lid. O-ring (**b**, arrow) seals the assembled chamber (**c**). (**c**) Arrow indicating the slit, in which the larva is to be placed. (**d**) Larva placed in the slit of the plastic spacer. Next, (**e**) the entire chamber is put on the microscope and connected to the vaporizer and the air supply (arrows). The tube connected to the outlet of the chamber (arrowhead) leads into a glass of water (not shown). (**f**–**k**) The imaging chamber is assembled as illustrated. First, the plastic spacer (**g**, olive part) and the Plexiglas guide ring (**g**, pink part) are placed in the modified Petri dish (**g**, orange part). Second, the larva is placed in the slit of the plastic spacer (**g**, blue arrowhead). Third, the cover slip (**f**, blue part) and the metal ring (**f**, gray part) are placed on the plastic spacer (**i**, olive part). Fourth, the lid (**h**) is placed on the chamber. The assembled chamber is shown in a side (**j**) and a 3D (**k**) view. (**l**) Pressurized fresh air (green arrows) enters the anesthetization device via inlet A (green star). Valve A (green arrowhead) and the anesthetic outlet (red dot) are opened to initiate anesthetization; valve B (blue arrowhead) and fresh air outlet (blue dot) are closed. Thus, the air (orange arrow) passes the anesthetization chamber (open triangle) where it is saturated with desflurane. Arrows indicating the flow direction point in direction of the imaging chamber. All valves and outlets are closed during imaging. The larva is recovered by opening valve B and the fresh air outlet. Fresh air (blue, green) and anesthetic (red) pressures can be adjusted at the respective valves (rectangles). Anesthetic stored in the anesthetization chamber can be refilled via inlet B red star, (**l**) and (**m**). (**n**) The neuromuscular junctions (NMJs) on the abdominal muscles 26 and 27 are particularly suited for *in vivo* imaging. Segment A3 is shown. Here, a transmitted light image has been merged with a false color-coded, nonlinearly contrasted *z*-projection of Mhc-CD8-GFP-Shaker[5] expressing larva.

4| Place the plastic spacer (**Fig. 2a**, white arrow; **Fig. 2g**, olive part) onto the oil layer.
▲ CRITICAL STEP Do not place the spacer upside down in the oil. The air slots of the grid have to face upward. Correctly match the spacer and the size of the larvae. The height of the spacer should be roughly half the larval diameter. The width of the slit should be about two times the diameter of the larvae.

5| Put the larva with the ventral side facing the microscope objective in the chamber (to image NMJ 26 and 27) (see **Fig. 2d**; **Fig. 2g**, arrowhead).
! CAUTION Always use a brush (not a forceps) when handling a larva.

6| Insert the Plexiglas guide ring (**Fig. 2a**, white arrowhead; **Fig. 2g**, pink part) into the chamber.

7| Place a 22 mm × 22 mm cover slip (**Fig. 2f**, blue part) onto the spacer and use the metal ring (**Fig. 2a**, red arrowhead; **Fig. 2f**, gray part) to fix the position of the larva (partially assembled chamber see **Fig. 2i**).
▲ CRITICAL STEP The larva will be gently squeezed. Be careful not to rupture the fat body. If necessary, rearrange the position of the larva by carefully moving the cover slip back and forth with a brush.

8| Place the lid (**Fig. 2b** and **h**) on the chamber (closed chamber see **Fig. 2c,j,k**).

9| Place the chamber on the microscope (**Fig. 2e**).

Image acquisition: anesthetization of the larva ● TIMING **1–2 min**
10| Connect the two inlets of the chamber (**Fig. 2e**, arrows) with an appropriate anesthetization device/vaporizer (**Fig. 2l** and **m**).
! CAUTION Larvae are anesthetized at rather high desflurane concentrations to arrest the heartbeat[3]. Thus, carefully check that the microscope room is well ventilated. Be sure that there are no leaks and that the effective concentration of desflurane in the room-air never exceeds, what safety regulations allow! Only a very small total volume of desflurane is needed to anesthetize larvae. For safety reasons, the vaporizer should never contain more desflurane than needed for 1–2 d of imaging.

11| Immerse the other end of the tube attached to the chamber outlet (**Fig. 2e**, arrowhead) in a glass of water to check air-flow.

12| Open the valves (e.g., **Fig. 2l**, green arrowhead and red dot) controlling anesthetic flow into the chamber for ~5 s.
! CAUTION If no air bubbles ascend in the water, the chamber is leaky.

13| Close the valves for ~3 s.

14| Monitor residual larval movements in the microscope. Check both the heartbeat and the muscle movements. If necessary, repeat Steps 12 and 13 until anesthetization of the larva is complete, then close all valves and start imaging.
▲ CRITICAL STEP Any residual muscle movement or heartbeat indicates that the animal is not properly anesthetized. Complete anesthetization is absolutely necessary for high-resolution images. Anesthetization usually continues even after valves are closed. It ends when air is put through the chamber. Please note that the anesthetization time should normally not exceed 15–20 min.
? TROUBLESHOOTING

Image acquisition: imaging
15| Identify abdominal muscles 26 and 27 in segments A2 to A4 (see **Fig. 2n**).
▲ CRITICAL STEP In principle, any muscle can be used for imaging. We prefer muscles 26 and 27 that are directly beneath the cuticle. They are easy to identify and relocate for subsequent images in a time series. Furthermore, the imaging quality decreases with penetration depth. Thus, NMJ 6/7 (preferably used for histological and electrophysiological analysis, as they are among the most superficial junction in an open preparation) are among the least suitable NMJs for *in vivo* imaging. Nevertheless, many transgenic lines (e.g., Mhc-CD8-GFP-Sh and dlg-GFP, see **Fig. 1** and **Table 1**) express a sufficiently strong FP label to image NMJ 6/7.
? TROUBLESHOOTING

16| Follow option A for time series, or option B to perform a FRAP experiment.
(A) Imaging ● TIMING **15–20 min**
(i) Image the structure you are interested in (e.g., the entire NMJ).
▲ CRITICAL STEP To obtain maximal resolution, we currently use a ×63 oil 1.4 NA objective, pinhole 1.0 and a voxel size of 100 nm × 100 nm × 500 nm. The main limitation is the time during which the larva is properly anesthetized. Thus, adjust the frame size to cover the whole structure with one single frame. If possible, scan only the NMJ (a 256 × 1024 pixel scan is much faster compared to a 1024 × 1024 pixel scan). Choose bidirectional scan mode and a low pixel dwell time (e.g., 1–2 µs) and average two to eight times.
? TROUBLESHOOTING

BOX 1 | GENERAL ADVICE FOR FLUORESCENCE RECOVERY AFTER PHOTO-BLEACHING EXPERIMENTS

Record immediately a postbleach image to confirm that bleaching is complete and irreversible (e.g., the reversible fraction is much higher for yellow fluorescent protein compared to GFP) and that the protein was not just driven in a dark state[35].
Collect a prebleach series to estimate acquisition photo-bleaching (and correct for it).
Use >50 times higher laser power for bleaching compared to acquisition.
Avoid bleaching at wavelength <450 nm, as photo-toxicity is generally higher at lower wavelength.
Consider the bleaching profile along the optical axis: low numerical aperture (NA) illumination will result in homogenous illumination of the sample, high NA objectives in a double conical beam shape. More precise definition of the bleached volume along the optical axis can be achieved with multiphoton excitation.
Normalize your detectors to verify that they respond linearly to the amount of fluorescent signal. Many FPs have the tendency to multimerize. Especially, when expressed at high local concentrations (e.g., overexpressed and targeted to membranes), this might substantially distort the dynamics of the tagged protein.

Opening the pinhole during bleaching allows quantifying bleaching—especially along the optical axis—more accurately.

Be sure to use the appropriate model to describe fluorescence recovery after photo-bleaching (FRAP). Mostly there is no complete FRAP. Always consider the potential existence of an immobile fraction. As it is often not feasible in *in vivo* imaging (compare **Fig. 3f**) to obtain enough data-points for an accurate, detailed kinetic analysis, be aware of this limitation when using the data to draw conclusions. Usually, plotting data with $\mathbf{f}(t) = \mathbf{A}\,(\mathbf{1}-e^{-\tau t})$ gives a reasonable good fit. **A** is the mobile fraction of the protein and thus determines the maximal FRAP. If, for example, 20% of the protein (**1–A**) are immobile, **A** is 0.8 and the maximal recovery will by 80% of the prebleach intensity. The half-life time $\tau_{1/2}$ is by definition the time when recovery is half of **A**. The recovery time constant τ is thus $\tau = -(\ln 0{,}5/\tau_{1/2})$.
We recommend refs. 36 and 37 for further reading.

(B) Bleaching for FRAP experiments ● TIMING **15–20 min**

(i) Obtain a prebleach image (Step 16(A)).
(ii) Adjust the zoom to select the region to be bleached or use the 'region of interest' (ROI) function of your microscope.
(iii) Change the laser power to 100% and bleach the selected region until $<10\%$ of the original signal is left.
▲ CRITICAL STEP To avoid bleaching outside the selected area, limit the bleaching to the minimal time necessary to obtain sufficient bleaching in the area of interest.
? TROUBLESHOOTING
(iv) Note the time when you finished bleaching.
(v) Record immediately a postbleach image to document bleaching efficacy. If feasible, use exactly the same settings used for the prebleach image.
(vi) If there is sufficient time between two time points in a time series, let larva recover from anesthetization (Steps 17–24).
▲ CRITICAL STEP When recording very fast time series (e.g., an image every minute), note that the anesthetization time should normally not exceed 15–20 min. Please note that volatile anesthetics like isoflurane (and likely also desflurane) seem to work by a slowing of action potentials and a decrease in presynaptic release. How this effect is mediated is still under debate. Thus, please consider this issue when studying presynaptic release during continuous anesthetization.
(vii) Repeat Steps 2–16 to record all other time points to monitor the recovery of the fluorescence. If possible, use exactly the same settings used for the prebleach image.

Image acquisition: recovery from anesthetization ● TIMING **2–5 min**

17| After imaging is completed, let air into the chamber (e.g., by opening valve B and the fresh air outlet; **Fig. 2l**, blue arrowhead and blue dot).

18| Monitor waking up of the larva by transmitted halogen light. Check heartbeat and muscle contractions.
▲ CRITICAL STEP Typically, first the heart starts to beat, next the muscles contract, and then the animal starts to move. Now, the animal can be removed from the imaging chamber (Steps 20–24).

19| Repeat Steps 17 and 18 until the larva wakes up.
▲ CRITICAL STEP If the heart does not start to beat within 2 min, the animal was anesthetized for too long and is likely dead. We thus stop any attempts to reanimate the animals after 2 min, provided we observe no signs of recovery from anesthetization (e.g., heartbeat, muscle movements).

20| Detach the chamber from the anesthetization device and remove it from the microscope.

21| Disassemble the chamber carefully.

22| Remove the cover slip, take the larva out and briefly rinse it with water.

23| Place the larva in a Petri dish, containing mashed fly cultivation medium.

24| Store the dish in an incubator at the appropriate temperature.

Image processing and quantification

25| Process and quantify the data. Follow option A (single channel) or option B (multichannel) to generate *z*-projections of 3D data sets. Follow option C for manual quantification of FRAP, option D for segmentation and quantification of small structures, or option E to trace the growth of individual synapses. Option F describes the semi-automated quantification of two-color FRAP.

(A) Standard processing of images ● TIMING 10 min per *z*-stack

(i) If necessary, export your raw data from the image acquisition software. Store each individual plane of a *z*-stack as a separate TIF file.

(ii) Import the raw data (*Import/Image sequence*).

(iii) Mark (freehand selections) and measure (*Analyse/Measure*) a representative area as background.
▲ CRITICAL STEP Make sure that what you select is really 'background' (e.g., by comparison with the background in tissues in which the protein of interest is not expressed) and does not represent diffuse pools of your protein of interest, for example, in the muscle.

(iv) Subtract the mean background intensity from every plane of the *z*-stack (*Process/Math/Subtract*).

(v) Apply Gaussian blur filtering (pixel radius = 1) to the *z*-stack (*Process/Filters/Gaussian Blur*).
▲ CRITICAL STEP Sometimes, it might be necessary to increase the radius to 2, but try to avoid this because it leads to more blurring of the image.

(vi) Decide which *z*-planes to include in the projection.
▲ CRITICAL STEP When analyzing NMJs, make sure to include all *z*-planes of the relevant area. If you have no *z*-planes above and below the area you want to study (which prove that the area was correctly imaged), discard the time series. Do not include the *z*-planes above and below the junction in the projection, they just add up to the noise.

(vii) Generate a projection (*Image/Stacks/Z-Project*).
▲ CRITICAL STEP Typically, morphological details are easier to discern in maximum projected data, while sum or average projections are better suited for accurate quantifications as they represent the entire protein population present in a given volume.
? TROUBLESHOOTING

(B) Processing of multicolor images ● TIMING 10–30 min per *z*-stack

(i) Perform Step 25A for each channel separately and merge the separate channels if desired (*Image/Color/RGB merge*).
▲ CRITICAL STEP Include the same set of *z*-planes for each channel.

(C) Manual quantification of FRAP ● TIMING 10 min to several hours per time-series

(i) Once the image has been processed as described in Step 25A for each individual time-point mark (freehand selections) and measure (*Analyse/Measure*) an appropriate not bleached control region (NBC) (e.g., **Fig. 3a**, yellow area).
▲ CRITICAL STEP If the protein is diffusely distributed (especially along the *z*-axis), do not use maximum projections. Maximum projections consider for each position in *x*/*y* only the information from the focal plane that has the highest pixel intensity. Average or sum projections avoid this problem. The control region must not be directly adjacent the 'bleach boundary'.

(ii) Mark (freehand selections) and measure (*Analyse/Measure*) an appropriate background control (BGC) region (e.g., **Fig. 3a**, cyan area).
▲ CRITICAL STEP Make sure that what you select as background is really 'background' and does not represent diffuse pools of your protein of interest, for example, in the muscle. If you decide to define diffuse pools of your protein of interest as background (which is for certain applications the appropriate control), state it explicitly. Typically, use a rather large area as BGC. The control region should neither be directly adjacent to the bleached area nor to the NMJ, nor to any source of unspecific signal.

(iii) Mark (freehand selections) and measure (*Analyse/Measure*) an appropriate ROI (e.g., **Fig. 3a**, red area).
▲ CRITICAL STEP The ROI must not be directly adjacent to the 'bleach boundary'.

(iv) Repeat Step 25C(i–iii) for all time-points. Measure at each time-point the area and the mean intensity.
▲ CRITICAL STEP If image acquisition and processing were correct, the mean value for background corrected control region (NBC-BGC) should not vary by >20%. If the regions were correctly re-identified, the area should not vary by >20%.
? TROUBLESHOOTING

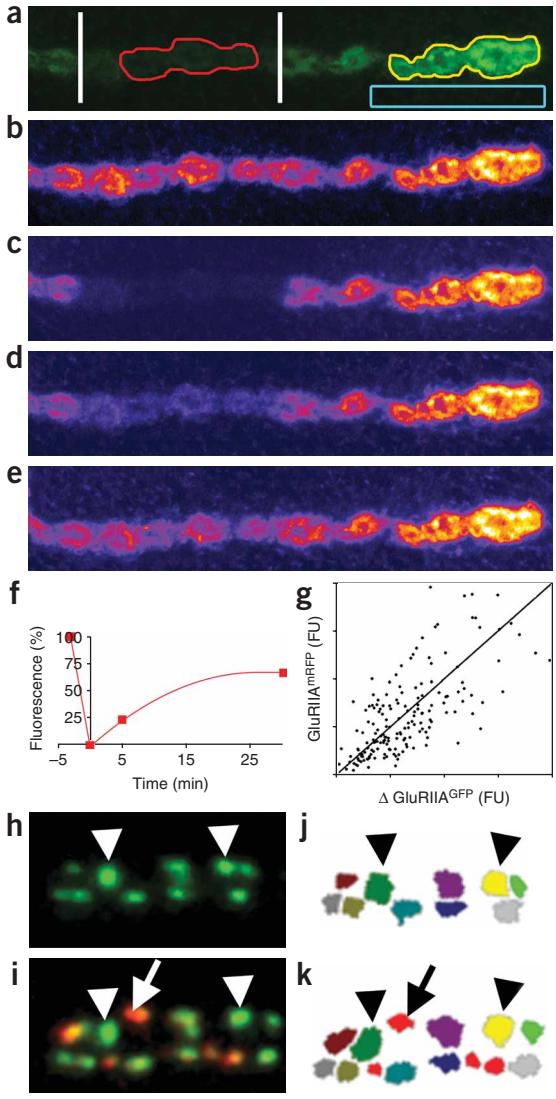

Figure 3 | Quantification of fluorescence recovery after photo-bleaching (FRAP). (**a**) Neuromuscular junction (NMJ) of a larva expressing S97-dlg-GFP[20] induced by C57-Gal4 5 min after bleaching S97-dlg-GFP. White vertical lines indicate the boundaries of the bleached area. Regions used for one-color FRAP-quantification are color-coded: yellow area: nonbleached control region, cyan area: background control region; note that here the diffuse, muscle wide pools of S97-dlg-GFP were used as background. This figure is only for illustration purposes. Usually, we select a substantially larger area as background reference, which is also more distant to the NMJ (compare Step 25C(ii)) red area: region of interest (ROI), here: bleached boutons. (**b**–**e**) The complete time-series of the FRAP experiment described in (**a**) using a different color lookup table (LUT). The time points are as follows: (**b**) before bleaching, (**c**) 0 min (i.e., directly after bleaching), (**d**) 5 min, (**e**) 30 min after bleaching. Note that slight differences in intensity are better recognized by the human eye when using the fire LUT compared to a single-color LUT (**a** and **d** show exactly the same image). (**f**) Quantification of the FRAP experiment shown in (**b**–**e**). (**g**) Receptor entry (GluRIIA^{mRFP} FRAP) at individual postsynaptic densities (PSDs) versus change in GluRIIA^{GFP} signal representing PSD growth over 24 h. FU: arbitrary fluorescence units. (**h**–**k**) Visualizing the entry of new GluRIIA receptors using FRAP. (**h**) PSDs expressing GluRIIA^{GFP} at $t = 0$ h. (**i**) 24 h after bleaching, the recovery of GluRIIA^{mRFP} is restricted to PSDs, which either formed newly (arrow and red in panel **k**) or which increased size. Stable synapses show no incorporation of GluRIIA^{mRFP} (arrowheads) (**j**,**k**): Exemplary segmentation masks used for quantification, newly formed PSDs (compare **h** and **i**) in red. ((**h**),(**i**) adapted from ref. 3).

(v) Calculate relative fluorescence (RF) in the ROI using the following formula:

$$RF[t] = \frac{(ROI[t] - BGC[t])}{(NBC[t] - BGC[t])}$$

(vi) Calculate the normalized RF (NRF) in the ROI using the following formula:

$$NRF[t] = \frac{RF[t]}{RF[t = \text{prebleach}]}$$

(vii) Plot and analyze the FRAP data in the software of your choice (see **Fig. 3f**).

(D) Segmentation and quantification of small structures

● TIMING **10 min to several hours per *z*-stack**

(i) Process the image as described in Step 25A and rescale the image by the factor of 2 (*Image/Scale*).

▲ CRITICAL STEP Maximum projections are more suitable for segmentation. Very small synapses are often obscured in average projections. Thus, we recommend not to use average projections in this step.

(ii) Obtain a binary mask, in which the structures of interest are set to 255 and the background to 0 (*Image/Adjust Threshold/→Apply*).

▲ CRITICAL STEP Using an appropriate threshold makes it possible to segment most structures automatically. When automatically segmenting closely spaced structures (e.g., synapses), the segmentation has to be manually corrected afterward (see next step). The fluorescence intensity between two large, bright synapses in close proximity is often higher than the intensity in the center of a small, dim (nascent) synapse. Choose a sufficiently low threshold to ensure that small synapses are not excluded from the analysis.

(iii) Set color picker to 0,0,0.

(iv) Select freehand line mode.

(v) Set line width to 2.

(vi) Manually segment the image by drawing (*Edit/Draw*) appropriate freehand lines. This image will be referred to as Image1 in Step 25D(viii).

▲ CRITICAL STEP The accuracy of your measurement will critically depend on the accuracy of your freehand lines. When the fluorescent intensity in the middle of an object is significantly lower than observed for two peaks of intensity located outside the center of the object, assume that two synapses are present. Use the 'intensity valley' between the two peaks to further segment the synapse.

? TROUBLESHOOTING

(vii) Reprocess the raw data by applying Step 25D(i). Usually, it is best to use average projection in Step 25A(vii). This image will be referred to as Image2 in the next step.
(viii) Using the Image Calculator function, write the original pixel intensities back into the segmented image (*Process/Image Calculator/Operation Min*, Image1 = Image1, Image2 = Image2). The resulting image will be referred to as Image3 in the next step.
(ix) Threshold Image3: Lower Threshold = 1 Upper Threshold = 255 (*Image/Adjust Threshold/→Set*)
(x) Set measurements (*Analyse/Set measurements*).
▲ CRITICAL STEP Do not forget to mark all values you are interested in. We usually determine area, mean grey value and circularity. Limit to threshold.
(xi) Analyze particles (*Analyse/Analyses Particles*).
▲ CRITICAL STEP The exact settings depend on the biological question you are interested in. We usually exclude residual noise by adjusting the Minimal particle size, Exclude on Edges, Display results and Show outlines.
(xii) For reference, print 'Drawing of Image3'.
(xiii) Paste results from Step 25D(xi) into, for example, Excel for analysis (Microsoft).

(E) Tracing the growth of individual synapses ● TIMING Several hours per time-series

(i) Process all time-points as described in Step 25D.
(ii) Identify synapses that are stable between two consecutive time-points (compare arrowheads in **Fig. 3h–k**).
(iii) Use these landmark synapses to identify all other synapses in the vicinity.
(iv) Mark all new synapses (**Fig. 3i** and **k** arrow and red synapses in **Fig. 3k**).
(v) Assign to every synapse a unique identifier. Make a table that contains all parameters that were determined for each synapse at each imaging time-point.
(vi) Use this table to quantify the parameter you are interested in.
▲ CRITICAL STEP The exact calculation as well as appropriate normalization will depend on the biological question you are interested in. As exemplified in **Figure 3g**, we quantified receptor incorporation after two-color FRAP.

(F) Semi-automated quantification of two-color FRAP ● TIMING Several hours per time-series (excluding Step 25F(i–ii))

(i) Tag the protein of interest with two different fluorophores (FP1) and (FP2) (e.g., GFP and mCherry). Establish the corresponding transgenic animals.
▲ CRITICAL STEP While it is possible to attach two fluorescent tags to a single protein, we recommend tagging one fraction of the protein population with FP1 and another fraction with FP2. In order to do this, two independent transgenic lines have to be established and crossed. In the progeny, offspring carrying both insertions have to be selected (next step).
(ii) Select and prepare the larva for *in vivo* imaging (Steps 1–14).
(iii) Record a FRAP time series following Step 25B, but bleach only one of the two FPs.
▲ CRITICAL STEP Be careful as to bleach only one FP.
? TROUBLESHOOTING
(iv) To monitor (e.g., receptor-dynamics) proceed as follows: process the nonbleached reference channel as described in Step 25E(i–v) and save Image1 in Step 25D(vi) as mask that will be used in Step 25F(vi).
(v) Process the raw data of the bleached channel by applying Step 25D(i). Usually, it is best to use average projection in Step 25A(vii). This image will be referred to as 'Bleached Channel' in Step 25F(vii).
(vi) Load the saved mask from Step 25F(iv).
(vii) Write the pixel intensities of the bleached channel into the segmented image. The resulting image will be referred to as 'Bleached Image3' in next Step (*Process/Image Calculator/Operation Min*, Image1 = Bleached Channel, Image2 = Mask).
▲ CRITICAL STEP This kind of processing can only be used when both channels are perfectly co-localized. As in the case of $GluRIIA^{GFP}$ and $GluRIIA^{mRFP\,3}$.
(viii) Threshold Bleached Image3: Lower Threshold = 1, Upper Threshold = 255 (*Image/Adjust Threshold/→Set*).
(ix) Set measurements and analyze particles as described in Step 25D(x and xi).
(x) Paste results into Excel, where already the reference channel data were stored in Step 25F(iv).
(xi) Appropriately compute the data as to extract the information you are interested in.
▲ CRITICAL STEP Normalize data if necessary. If feasible, include nonbleached control synapses as reference. The FP1/FP2 ratio in the bleached area compared to a nonbleached control can be used to quantify local protein dynamics, as well as to trace the origin of the protein inserted into the structure of interest.

● TIMING

Steps 1–9, assemble the imaging chamber: 5 min per larva
Steps 10–14, anesthetization: 1–2 min per larva
Step 16A, imaging: 3–5 min per NMJ/15–20 min per larva
Step 16B, bleaching for FRAP experiments: 10 min per NMJ
Steps 17–19, recovery from anesthetization: 2 min per larva

Steps 20–24, disassembly of the imaging chamber: 2–3 min
Step 25A, standard processing of images: 10 min per *z*-stack
Step 25B, processing of multicolor images: 10–30 min per *z*-stack
Step 25C, manual quantification of FRAP: 10 min to several hours per time-series
Step 25D, segmentation and quantification of small structures: 10 min to several hours per *z*-stack
Step 25E, tracing the growth of individual synapses: several hours per time-series
Step 25F, semi-automated quantification of two-color FRAP: 30 min to several hours per time series

? TROUBLESHOOTING

General advice on how to conduct FRAP experiments can be found in **Box 1**. Troubleshooting advice can be found in **Table 3**.

TABLE 3 | Troubleshooting table.

Step	Problem	Possible reasons: How to check?	Solution
14	Anesthetization fails	Chamber is leaky: Do air bubbles ascend in the water? No →	 Reassemble chamber Build new chamber
		Posterior parts of the trachea of the larva covered with oil	Wash larva Use other larva
		Room temperature too high	Ideal room temperature for anesthetization is 20 ± 1 °C
15	Failure to re-identify junctions	Lack of training	Train with larvae in which the muscles are brightly stained (Mhc-CD8-GFP-Shaker[5]). Take overview pictures at lower magnification
		The segment is contracted and thus optical access is bad	Let larva recover from anesthetization and anesthetize it again
		The junction was bleached during the previous imaging time-points	1. Always verify that you do not bleach substantially during acquisition. 2. Do two successive *z*-stack scans of the same neuromuscular junction (NMJ) using exactly the same settings. Second image should at least have 80% of the signal left. Use these settings for future experiments
16A(i)	Signal is too weak	Signal is really too weak for your setup	1. Use more superficial junctions 2. If possible, open pinhole to 1.5 or 2 airy units. Enhance detector gain to the limit of what is reasonable (i.e., not more noise than can be compensated for) and compensate for noise by averaging. 3. Make new transgenic constructs with better expression
		Need to buy a more sensitive microscope	There are many factors that determine the 'observed' sensitivity of a microscope. To compare the sensitivity of two different microscopes, choose settings that will provide you with the same image quality (also in respect to cross-talk) and signal-to-noise ratio (at rather high PMT gain, low laser power and fast scan speed) at both microscopes. Then image the same structure five times. The drop in fluorescence caused by bleaching is a good measure for the sensitivity of the microscope (in simplified terms: the higher the sensitivity, the less photons need to be exited to obtain a high quality image. The less photons are exited, the lower is the chance for bleaching)
		Optical access is not good	Remount larva, check: Is oil film ok? Is the larva nicely flattened? Is the segment not contracted?

TABLE 3 | Troubleshooting table (continued).

Step	Problem	Possible reasons: How to check?	Solution
16A(i)	Signal is too weak	Bleaching while searching for the junction	Open the pinhole and reduce the laser-power while searching for a junction
	Larva wakes up before you have finished acquisition or dies due to too prolonged anesthetization	Image acquisition takes too long	Train to be faster in identifying junctions. Increase speed of image acquisition (pixel dwell time, image size, minimal number of *z*-planes)
16B(iii)	Bleaching takes too long		Use stronger laser, especially the commonly used 543 HeNe might be too weak for fast bleaching of strong red fluorescent protein signals. Use instead a 10-mW solid state yellow laser (561 nm)
25A(vii)	Structures that are above or below the NMJ obscure in the projected image parts of the NMJ		If the structures are indeed clearly separate from the NMJ (like trachea) remove them in the respective *z*-planes using the freehand selection tool *Note:* Some journals might consider such manipulations (even when properly done) as scientific misconduct. Therefore, always clearly state how you processed the raw data, and present the unprocessed raw data to reviewers/editors or include them as supplementary figures. *Note:* Make sure that the 'manipulated' projection accurately represents the information contained in the raw data
	Small dim structures like new postsynaptic densities (PSDs) are difficult to discern in your images		Use a multicolor LUT for example, fire (compare **Fig. 3b–e**) Adjust gamma (*Process/Math/Gamma*) *Note:* Some journals require that you specify such adjustments. Even if it is not asked for, clearly state how you processed the raw data
25C(iv)	Control region varies by >20%	Do you bleach during image acquisition? Yes →	Optimize acquisition (see Troubleshooting Step 15) and start new time series
		Does the optical access vary? Yes→	Ensure that the larva is always correctly mounted
	Area varies by >20%	Was processing OK? No →	Redo processing Use appropriate thresholds or be more careful when drawing the freehand sections
		Did the structure really grow? Yes→	Then just ignore the variation and proceed with the processing
25D(vi)	One area is very difficult to segment		Exclude this area from the analysis, but make sure to do this in a nonbiased way, when comparing (e.g., different genotypes) *Note:* Always state that data were excluded from analysis, why and on basis of which criteria.
	Difficulties in deciding 'whether the fluorescent intensity in the middle of an object is significantly lower than observed for the two peaks of intensity located outside the center of the object'		Select five examples for which it is reasonable to assume that two different structures are present (based on 3D information from the original *z*-stack). Next, select *straight line mode*. Draw a line that connects both peaks and plot a profile (*Analyse/Plot Profile*). Extract from the profile the intensity of the peaks and the intensity of the 'valley'. Average the 'valley to lower peak' ratio for the five measurements. Use this ratio (e.g., 0,6) as cut-off to

TABLE 3 | Troubleshooting table (continued).

Step	Problem	Possible reasons: How to check?	Solution
			decide whether the fluorescent intensity in the middle of an object is significantly lower than observed for the two peaks of intensity located outside the center of the object
25F(iii)	Bleaching of both fluorescent proteins (FP) occurs		Select an appropriate pair of FPs that has no excitation cross-talk at the wavelength you plan to use for bleaching (e.g. EGFP and mRFP, bleach at 561 nm)

ANTICIPATED RESULTS

Anticipate results you did not anticipate! Spilt-like redistributions of glutamate receptors from the existing postsynaptic densities (PSDs) into new PSDs were postulated as the basic mechanism for synapse formation in the mammalian CNS[12]. Thus, we set out to prove by *in vivo* imaging, that new PSDs are indeed formed by the split of existing ones. While we found no convincing evidence to prove that point, we could show that new PSDs largely—if not exclusively—form *de novo*[3]. Furthermore, we could show that glutamate receptors in our intact preparation are characterized by the mean synaptic residence times of many hours[3], while results from cell culture suggested that the residence times should be in the time scale of minutes[13]. Nevertheless, it is necessary to have some reasonable assumption about the timing of biological processes you are about to study. It is obvious that large rearrangements of structures, such as the formation of new boutons, are likely to take longer than the slight movement of a fast axonal cargo. Membrane-bound molecules (e.g., Fascilin2) or receptors (e.g., glutamate receptors) are generally exchanged much slower compared to synaptic vesicles or synaptically localized, cytosolic proteins, such as p21-activated kinase PAK (compare **Fig. 4a**).

During image acquisition and while analyzing the data, care has to be taken, neither to affect biological processes with the imaging procedure nor to misinterpret the results. First, the animal must not be harmed during the imaging procedure. Negative effects on larval development can be caused by extended anesthetization periods. Oil that enters into the tracheal system due to improper handling of the larva will subsequently hinder breathing. The fat body (or other organs) can be damaged mechanically when mounting the larva. Fat body damage will usually result in the death of the larva several hours after the insult. Thus, appropriate criteria have to be met to monitor the 'health status' of the larva. Rapid recovery from anesthetization, as well as immediate movement (including feeding), is the most reliable criteria. If larval development is imaged for several hours or days, increase of body length is a good indicator for undisturbed development.

Second, as irradiation of fluorophores creates reactive oxygen species, it is a general concern that bleaching might cause functional inactivation of the proteins. Thus, tests on whether the bleaching of glutamate receptors influences their functionality were undertaken. The fact that evoked NMJ currents were indistinguishable before and after completely bleaching all synaptic GFP signal[3] indicates that the protein of interest should not be affected by bleaching the GFP attached to it. However, it might be necessary to verify this fact if possible for each protein to be studied.

Third, care has to be taken to correctly re-identify the individual structures at various time-points. The choice of appropriate landmarks helps to avoid intermixing different structures. When imaging GFP-tagged glutamate receptors[3], we recognized that the PSDs, which were established at the beginning of a time-series (**Fig. 4b**, arrowheads), showed only little change over time. Thus, these PSDs are suitable 'landmarks' to relocate and monitor a certain synaptic population.

Fourth, the limited temporal and spatial resolutions have to be taken into consideration before drawing any conclusions. As limited temporal and spatial resolutions are a typical problem to be faced in *in vivo* imaging, we will discuss what led us to the conclusion that new PSDs are largely—if not exclusively—formed by *de novo* formation[3]. Morphological imaging allows only visualizing structures at defined time-points (e.g., every 12 h, compare **Fig. 4b**). We observed that new PSDs form predominantly distant (**Fig. 4b**, white arrows) from the pre-existing PSDs, suggesting that they form independent from neighboring PSDs. However, we could not exclude that new PSDs form by a splitting or budding mode that is very fast (e.g., in the time scale of minutes). Thus, even if we were to image every hour, we could still have missed all the split events. With the current protocols, it is impossible to image every minute for several days. Next, the diffraction limit of the microscope has to be considered, especially when closely spaced, small ($<$500 nm) structures, such as components of the PSD or the presynaptic active zone (such as Bruchpilot[10]), are imaged. In time-series of PSD development situations were observed, which at first glance mimicked potential splitting processes (**Fig. 4b**, white circle). However, one has to be aware that, as simulated in **Figure 4c,** a *de novo* formation of a small synapse in close proximity ($<$200 nm) of a large one is not discernable as such. Such closely spaced PSDs can only be clearly identified as separate entities when they have increased the distance to one another, because the presynaptic bouton they are located on has grown (**Fig. 4b**, white circle). Consistently, new PSDs can be observed, which form close to established PSDs (**Fig. 4b**, blue arrow, central panel). As they grow, these PSDs sometimes reach a density at which individual PSDs can no longer be identified as such (**Fig. 4b**, blue arrow, right panel). Tracing the molecular composition of cellular structures (such as synapses) using two-color FRAP is found to be the best way to finally clarify these questions[3].

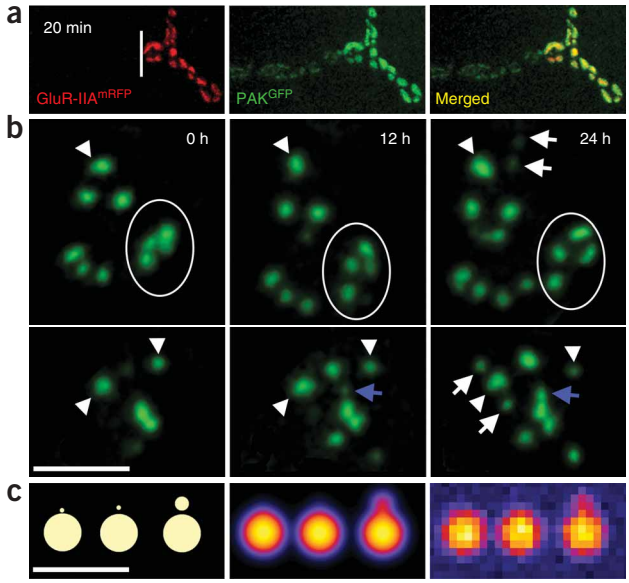

Figure 4 | Anticipated results. (**a**) Postsynaptic density (PSD) component p21 activated kinase PAK shows fast turnover. *In vivo* fluorescence recovery after photo-bleaching (FRAP): confocal time-series of a GluR-IIA^{mRFP} (red) and PAK^{GFP} (green) expressing junction. The area left of the vertical line was bleached. After 20 min, substantial FRAP of PAK^{GFP} is visible while no FRAP of GluR-IIA^{mRFP} is visible. (**b**) Time-series of dynamic changes at identified populations of PSDs (GluR-IIA^{mRFP}) shown in high magnification. Newly appearing PSDs are marked by arrows; PSDs present at the start of observation ($t = 0$ h), which were used as 'landmarks' are indicated by arrowheads. White circles (upper panel) label an area where PSDs increase distance over time. White arrows label PSDs, which form distant from pre-existing PSDs. The blue arrows (lower panel) show an example of two PSDs, which are so close together after outgrowth, that they can no longer be separated by confocal microscopy. Scale bar is 4 μm. (**c**) Here the point-spread function of a confocal microscope was applied to hypothetical intermediates of PSD formation. The theoretical image in the left panel was the source image for the calculations shown in the central panel after applying the point spread function of the microscope. For this calculation, a pixel size of 2 × 2 nm^2 was used. The results of the calculations are shown in the pixel size used for *in vivo* imaging in ref. 3 (98 × 98 nm^2). Here it is clearly impossible to differentiate two PSDs in close proximity. Scale bar is 1.25 μm. (Panels **a** and **b** are adapted from ref. 3).

In certain applications, stimulated emission depletion microscopy[14,15] might be very helpful when discerning, whether a certain structure actually represents one or two distinct synapses.

Last, the NMJ is a highly dynamic structure. It is located on a muscle, and the exact spacing of synapses might even depend on the degree of muscle contraction. Therefore, it is best not to image contracted segments and muscles. Additionally, much care has to be taken that growth or some reorganization of bouton structures, during which individual synapses move slightly, are not mistakenly used to state that synapses fuse or split, appear or disappear. Whenever new formation is scored, the rate of disappearing synapses also has to be quantified, and a decision has to be made whether synapses indeed did disappear or whether they just came in such close proximity, that they can no longer be identified as distinct entities.

Although the development of the nervous system is inherently a process of dynamic change, until recently it has mainly been investigated by interference from static images. While first advances gave some insights in long-standing questions of neuronal development, main technical issues remained to be addressed. Limited sensitivity leads researchers to overexpress their constructs rather than expressing them at physiological levels or to study synapse formation in culture rather than *in vivo*. Until very recently, lack of spatial resolution along with a lack of appropriate transgenic animals made it virtually impossible to study synaptic components (e.g., PSD-95)[2] rather than morphological correlates (e.g., spines) *in vivo*. Our protocol for *in vivo* imaging addressed some of these issues. Clearly, imaging the molecular composition of synapses *in vivo* in even more detail, using the powerful genetics of *Drosophila* and benefiting from the rapid pace of molecular and optical innovations, will help to clarify many open questions that could not be answered with static images. Thus, we fully agree with what Yogi Berra once said: 'you can observe a lot just by watching'[16].

Note: Supplementary information is available via the HTML version of this article.

ACKNOWLEDGMENTS We thank Yvonne Eisele and Wernher Fouquet for comments on the manuscript. We thank Andreas Schönle and David Sandstrom for technical advice. We thank Hubert Willmann for the mechanical drawings, and Frank Kötting for constructing the imaging chamber and the anesthetization device. We thank Michael Knopp, as well as all other laboratory and mechanics workshop members, for help and discussion. This work was supported by grants from the University of Tübingen (fortüne 1691-0-0 and fortüne 1626-0-0) and from the Landesstiftung Baden-Württemberg to T.M.R.

Published online at http://www.natureprotocols.com
Reprints and permissions information is available online at http://npg.nature.com/reprintsandpermissions

1. Walsh, M.K. & Lichtman, J.W. *In vivo* time-lapse imaging of synaptic takeover associated with naturally occurring synapse elimination. *Neuron* **37**, 67–73 (2003).
2. Gray, N.W., Weimer, R.M., Bureau, I. & Svoboda, K. Rapid redistribution of synaptic PSD-95 in the neocortex *in vivo*. *PLoS Biol.* **4**, e370 (2006).
3. Rasse, T.M. *et al.* Glutamate receptor dynamics organizing synapse formation *in vivo*. *Nat. Neurosci.* **8**, 898–905 (2005).
4. Sigrist, S.J., Reiff, D.F., Thiel, P.R., Steinert, J.R. & Schuster, C.M. Experience-dependent strengthening of *Drosophila* neuromuscular junctions. *J. Neurosci.* **23**, 6546–6556 (2003).
5. Zito, K., Parnas, D., Fetter, R.D., Isacoff, E.Y. & Goodman, C.S. Watching a synapse grow: noninvasive confocal imaging of synaptic growth in *Drosophila*. *Neuron* **22**, 719–729 (1999).
6. Rasse, T.M. *In Vivo Imaging of Long-term Changes in the Drosophila Neuromuscular Junction* Dissertation. Göttingen, Germany: Ernst-August University (2004).
7. Qin, G. *et al.* Four different subunits are essential for expressing the synaptic glutamate receptor at neuromuscular junctions of *Drosophila*. *J. Neurosci.* **25**, 3209–3218 (2005).
8. Kawasaki, F., Zou, B., Xu, X. & Ordway, R.W. Active zone localization of presynaptic calcium channels encoded by the cacophony locus of *Drosophila*. *J. Neurosci.* **24**, 282–285 (2004).
9. Shaner, N.C., Steinbach, P.A. & Tsien, R.Y. A guide to choosing fluorescent proteins. *Nat. Methods* **2**, 905–909 (2005).
10. Wagh, D.A. *et al.* Bruchpilot, a protein with homology to ELKS/CAST, is required for structural integrity and function of synaptic active zones in *Drosophila*. *Neuron* **49**, 833–844 (2006).

11. Sandstrom, D.J. Isoflurane depresses glutamate release by reducing neuronal excitability at the *Drosophila* neuromuscular junction. *J. Physiol.* **558**, 489–502 (2004).
12. Carlin, R.K. & Siekevitz, P. Plasticity in the central nervous system: do synapses divide? *Proc. Natl. Acad. Sci. USA* **80**, 3517–3521 (1983).
13. Tardin, C., Cognet, L., Bats, C., Lounis, B. & Choquet, D. Direct imaging of lateral movements of AMPA receptors inside synapses. *EMBO J.* **22**, 4656–4665 (2003).
14. Kittel, R.J. *et al.* Bruchpilot promotes active zone assembly, Ca^{2+}-channel clustering, and vesicle release. *Science* **312**, 1051–1054 (2006).
15. Klar, T.A., Engel, E. & Hell, S.W. Breaking Abbe's diffraction resolution limit in fluorescence microscopy with stimulated emission depletion beams of various shapes. *Phys. Rev. E. Stat. Nonlin. Soft Matter Phys.* **64**, 066613 (2001).
16. Kasthuri, N. & Lichtman, J.W. Structural dynamics of synapses in living animals. *Curr. Opin. Neurobiol.* **14**, 105–111 (2004).
17. Zhang, Y.Q., Rodesch, C.K. & Broadie, K. Living synaptic vesicle marker: synaptotagmin-GFP. *Genesis* **34**, 142–145 (2002).
18. Wucherpfennig, T., Wilsch-Brauninger, M. & Gonzalez-Gaitan, M. Role of *Drosophila* Rab5 during endosomal trafficking at the synapse and evoked neurotransmitter release. *J. Cell Biol.* **161**, 609–624 (2003).
19. Pilling, A.D., Horiuchi, D., Lively, C.M. & Saxton, W.M. Kinesin-1 and Dynein are the primary motors for fast transport of mitochondria in *Drosophila* motor axons. *Mol. Biol. Cell* **17**, 2057–2068 (2006).
20. Bachmann, A. *et al.* Cell type-specific recruitment of *Drosophila* Lin-7 to distinct MAGUK-based protein complexes defines novel roles for Sdt and Dlg-S97. *J. Cell Sci.* **117**, 1899–1909 (2004).
21. Bobinnec, Y., Morin, X. & Debec, A. Shaggy/GSK-3beta kinase localizes to the centrosome and to specialized cytoskeletal structures in *Drosophila*. *Cell Motil. Cytoskeleton* **63**, 313–320 (2006).
22. Zhang, J. *et al.* Thirty-one flavors of *Drosophila* rab proteins. *Genetics* **176**, 1307–1322 (2007).
23. Grieder, N.C., de Cuevas, M. & Spradling, A.C. The fusome organizes the microtubule network during oocyte differentiation in *Drosophila*. *Development* **127**, 4253–4264 (2000).
24. Besse, F. *et al.* The Ig cell adhesion molecule Basigin controls compartmentalization and vesicle release at *Drosophila melanogaster* synapses. *J. Cell Biol.* **177**, 843–855 (2007).
25. Lee, T. & Luo, L. Mosaic analysis with a repressible cell marker for studies of gene function in neuronal morphogenesis. *Neuron* **22**, 451–461 (1999).
26. Yeh, E., Gustafson, K. & Boulianne, G.L. Green fluorescent protein as a vital marker and reporter of gene expression in *Drosophila*. *Proc. Natl. Acad. Sci. USA* **92**, 7036–7040 (1995).
27. Lin, D.M. & Goodman, C.S. Ectopic and increased expression of Fasciclin II alters motoneuron growth cone guidance. *Neuron* **13**, 507–523 (1994).
28. Luo, L., Liao, Y.J., Jan, L.Y. & Jan, Y.N. Distinct morphogenetic functions of similar small GTPases: *Drosophila* Drac1 is involved in axonal outgrowth and myoblast fusion. *Genes. Dev.* **8**, 1787–1802 (1994).
29. Aberle, H. *et al.* wishful thinking encodes a BMP type II receptor that regulates synaptic growth in *Drosophila*. *Neuron* **33**, 545–558 (2002).
30. Osterwalder, T., Yoon, K.S., White, B.H. & Keshishian, H. A conditional tissue-specific transgene expression system using inducible GAL4. *Proc. Natl. Acad. Sci. USA* **98**, 12596–12601 (2001).
31. Brand, A.H. & Perrimon, N. Targeted gene expression as a means of altering cell fates and generating dominant phenotypes. *Development* **118**, 401–415 (1993).
32. Davis, G.W., Schuster, C.M. & Goodman, C.S. Genetic analysis of the mechanisms controlling target selection: target-derived Fasciclin II regulates the pattern of synapse formation. *Neuron* **19**, 561–573 (1997).
33. Budnik, V. *et al.* Regulation of synapse structure and function by the *Drosophila* tumor suppressor gene dlg. *Neuron* **17**, 627–640 (1996).
34. Halfon, M.S. *et al.* New fluorescent protein reporters for use with the *Drosophila* Gal4 expression system and for vital detection of balancer chromosomes. *Genesis* **34**, 135–138 (2002).
35. Schwille, P., Kummer, S., Heikal, A.A., Moerner, W.E. & Webb, W.W. Fluorescence correlation spectroscopy reveals fast optical excitation-driven intramolecular dynamics of yellow fluorescent proteins. *Proc. Natl. Acad. Sci. USA* **97**, 151–156 (2000).
36. Axelrod, D., Koppel, D.E., Schlessinger, J., Elson, E. & Webb, W.W. Mobility measurement by analysis of fluorescence photobleaching recovery kinetics. *Biophys. J.* **16**, 1055–1069 (1976).
37. Rabut, G. & Ellenberg, J. Photobleaching techniques to study mobility and molecular dynamics of proteins in live cells: FRAP, iFRAP, and FLIP. In *Live Cell Imaging—A Laboratory Manual* (eds. Goldman, R.D. & Spector, D.) 101–127 (Cold Spring Harbor Press, Cold Spring Harbor, New York, 2005).